A&A manuscript no.
(will be inserted by hand later)

Your thesaurus codes are:
03.01.02, 03.19.1, 03.20.2

ASTRONOMY
AND
ASTROPHYSICS
23.2.1998

First statistical data on wavefront outer scale at La Silla observatory from the GSM instrument

F. Martin[1], **A. Tokovinin**[2], **A. Ziad**[1], **R. Conan**[1], **J. Borgnino**[1], **R. Avila**[1], **A. Agabi**[1], **and M. Sarazin**[3]

[1] U.M.R. Astrophysique N° 6525 - C.N.R.S. - Université de Nice-Sophia Antipolis, F-06108 Nice Cedex 2, France
[2] Sternberg Astronomical Institute, Universitetsky prosp., 13, 119899 Moscow, Russia
[3] European Southern Observatory, Karl-Schwarzschild-Str. 2, D-85748 Garching bei München, Germany

Received ... 1998; accepted

Abstract. Results of the first monitoring of the wavefront outer scale $\mathcal{L}_0$ during 16 nights at La Silla, Chile, are presented. This parameter is of importance for high angular resolution observing techniques like adaptive optics and optical interferometry. It was measured with the Grating Scale Monitor (GSM) instrument which is based on the analysis of the spatial covariance of angle of arrival fluctuations simultaneously detected at several points on the wavefront. The outer scale distribution is found to be log-normal, with median value of 24 m and rms scatter of $\log\mathcal{L}_0$ of ± 0.22. Short-duration bursts of $\mathcal{L}_0$ are noted. During 1 hour the $\mathcal{L}_0$ and seeing were simultaneously measured with the ADONIS adaptive optics system at the 3.6 m telescope, and a good agreement with our data was noted.

Our measurements of the seeing were found to agree with the ESO DIMM seeing data. Effective wavefront velocity was also found in order to estimate the adaptive optics time constant.

Key words: seeing – adaptive optics – interferometry

Fig. 1. View of the GSM instrument at La Silla. The central pier with two modules in differential configuration is seen on the left, the eastern module in the center and the southern module on the right.

1. Introduction

Substantial progress in astronomical imagery has been recently achieved due to the rapid development of high angular resolution (HAR) techniques like adaptive optics (AO) and long baseline optical interferometry (LBI). It is known that these techniques are severely influenced by atmospheric turbulence (Roddier 1981). To quantify atmospheric effects, it is necessary to know several parameters directly related to the wavefront structure, namely the Fried's parameter r_0 which defines the FWHM seeing angle $\beta = 0.98\lambda/r_0$, the characteristic time constant, the isoplanatic angle and the wavefront outer scale $\mathcal{L}_0$ (Borgnino 1990). This last parameter defines the maximum size of wavefront perturbations and is poorly known: values of $\mathcal{L}_0$ ranging from 2 m to 2000 m were published (Avila et al. 1997). Here we present the first large and homogeneous data set on $\mathcal{L}_0$ which permits the evaluation of the statistical behaviour of the outer scale at a major astronomical site.

Send offprint requests to: F. Martin

2. The GSM instrument: principle

The Grating Scale Monitor (GSM) can be considered as a Shack-Hartmann kind technique based on measurements of angle of arrival (AA) fluctuations at several points on the wavefront. A statistical analysis of the recorded AA is performed to estimate spatial and temporal wavefront parameters. The prototype version of the instrument is described by Martin et al. (1994), and the first $\mathcal{L}_0$ measurements were published by Agabi et al. (1995).

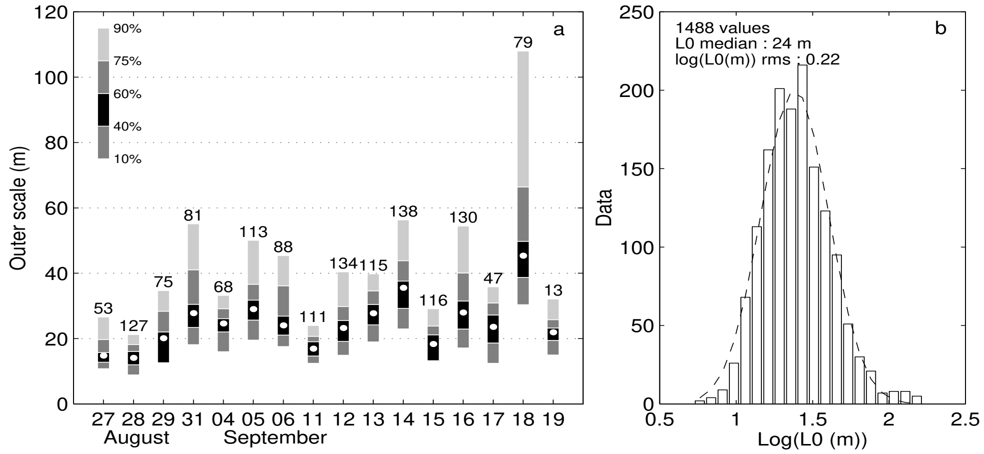

Fig. 4. Summary of the outer scale statistics over 16 nights. a) For each night the 5 levels of the cumulative distribution of $\mathcal{L}_0$ are shown by grey-scale bars, median values are plotted as circles. Total number of measurements for each night is indicated above the bars. b) Histogram of $\log \mathcal{L}_0$ for the whole mission with a fitted log-normal distribution (dashed line).

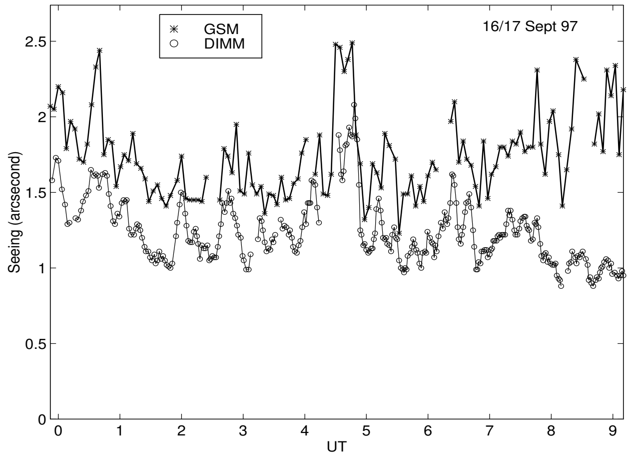

Fig. 2. Comparison of simultaneous seeing measured by ESO DIMM and by GSM

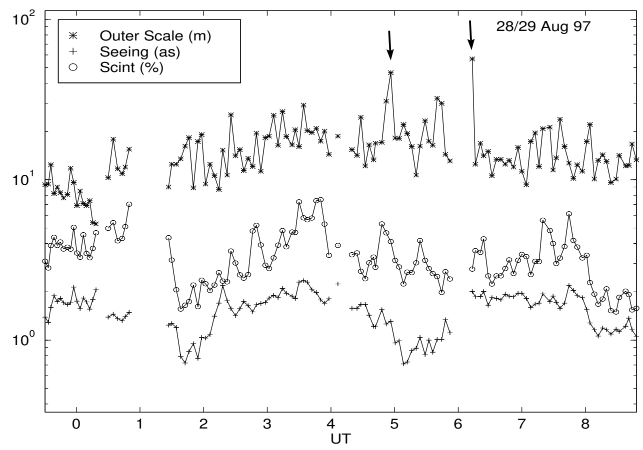

Fig. 3. Temporal evolution of $\mathcal{L}_0$, scintillation index and seeing (upper, middle and lower curves, respectively) during the night of August 28/29. Arrows indicate $\mathcal{L}_0$ bursts.

The instrument consists of four 10-cm telescopes on equatorial mounts (Fig. 1). Each telescope is equipped with a detection module which is capable of measuring synchronously the AA in the declination direction with a 5 ms sampling time. Two telescopes are installed on a common mount on the central pier and work as a differential image motion monitor (DIMM) (Sarazin & Roddier 1990) with a 25 cm baseline measuring r_0. Two other telescopes have separate mounts on separate piers, located 0.8 m to the south and 1 m to the east from the central pier, thus forming an L-shaped configuration. Telescope objectives were situated 1.5 m above the ground.

A typical measurement sequence consists of 2 mn data acquisitions repeated continuously every 4 mn. Pairwise telescope combinations provide 6 baselines ranging from 25 cm to 1 m. The AA covariances are computed for each baseline and normalized by the differential variance of AA on the 25-cm baseline. They are compared to Von Kàrmàn theoretical normalized covariances (Avila et al. 1997) and the appropriate $\mathcal{L}_0$ is found for each baseline. Before comparison, the baselines (length and orientation) are projected onto the wavefront plane. Final value of $\mathcal{L}_0$ is taken as a median of individual $\mathcal{L}_0$ values and its error is estimated from their scatter.

The $\mathcal{L}_0$ measured by GSM can be viewed as a parameter of Von Kàrmàn turbulence model which provides adequate description of wavefront structure at metric distances. It can be used to compute wavefront statistics over telescope aperture and is thus directly relevant to AO applications (Voitsekhovich & Cuevas 1995). On the other hand, estimates of the atmospheric phase fluctuations in LBI using $\mathcal{L}_0$ values found here are more model-dependent.

In order to check for wind shake effect, r_0 is computed from absolute image motion in each telescope, corrected for finite $\mathcal{L}_0$ (Borgnino et al. 1992) and compared to r_0 provided by the differential technique. A good agreement is found for ground wind speed less than 10 m/s, showing that telescope vibrations were not significant. Even at wind speeds up to 15 m/s GSM remains operational because vibrations of telescopes on separate piers are uncorrelated.

The scintillation index σ_I^2 is computed during data reduction and, as shown by Loos & Hogge (1979), it can give an estimate of the isoplanatic angle when the pupil diameter is around 10 cm. GSM data are also used to derive the effective wavefront speed and its direction (see below) which gives an estimate of the wavefront coherence time. So, this instrument can provide an almost complete set of wavefront parameters relevant to HAR techniques.

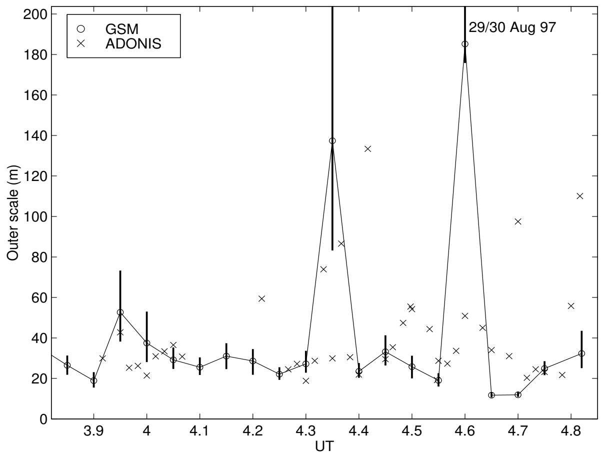

Fig. 5. Comparison of the outer scale values measured simultaneously using GSM and ADONIS. Error bars corresponding to $\pm\sigma$ are shown for GSM data.

3. GSM campaign at La Silla Observatory

Monitoring of turbulence parameters at La Silla observatory with GSM was organized in the framework of the ESO VLT Astronomical Site Monitor development program in August-September 1997. At this site the seeing is measured routinely with an automatic ESO DIMM (Sarazin & Roddier 1990) located on a tower 5 m above ground level. GSM has been installed close to ESO DIMM. During this campaign GSM data were obtained on 16 nights (a total of 115 hours of $\mathcal{L}_0$, seeing and scintillation measurements). Below we present the first results. The conditions of jet stream prevailed during our mission, the seeing being worse (median value 1.7 $''$) and more rapid than average for this season.

3.1. Seeing: comparison with ESO DIMM

It is interesting to compare the seeing measured simultaneously by GSM and ESO DIMM. Such comparison is given in Fig. 2 for one night with a moderate ground wind (10 m/s). There is a very good correlation between the seeing variations measured independently by the two instruments. Nevertheless, GSM measures seeing angles that are systematically greater than those given by ESO DIMM. This bias can be explained in part by the ground layer turbulence, and by the difference between integration times which are 5 ms and 10 ms for GSM and ESO DIMM, respectively. When the GSM integration time was artificially increased to 10 ms, a good agreement was obtained on nights with strong wind. A perfect agreement between GSM and ESO DIMM was found for the periods corresponding to very good seeing (0.6 $''$) and slow wind. On August 28/29, under atypical conditions of slow southern wind, the influence of surface layer turbulence was detected by comparing GSM and ESO DIMM data.

3.2. The wavefront outer scale statistics

Continuous monitoring of the outer scale enables us for the first time to study the temporal variation of $\mathcal{L}_0$ and its correlation with other seeing parameters. As an example, $\mathcal{L}_0$, σ_I^2 and seeing are plotted in Fig. 3 in a logarithmic scale as a function of time for one night. The temporal variation of $\mathcal{L}_0$ shows two characteristic features. First, slow trends with a time scale of hours are noted, just like for the other atmospheric parameters. Second, isolated values of large $\mathcal{L}_0$ are observed (arrows in Fig. 3, see also Fig. 5). This "bursts" of $\mathcal{L}_0$ are noted here for the first time. There are no matching rapid variations of seing or scintillation. Thus these bursts correspond only to the transient changes of wavefront spatial structure.

A positive correlation between $\mathcal{L}_0$ and seeing angle was found on some nights (e.g. on September 6/7 the correlation coefficient was $\rho = 0.55$) and was absent on other nights. The nightly median values of $\mathcal{L}_0$ and seeing do show some correlation ($\rho = 0.65$). Such a correlation is expected from the theoretical considerations.

In Fig. 4 the overall statistics of the outer scale is shown. For each night the few characteristic levels of $\mathcal{L}_0$ cumulative distribution and its median are plotted. The night-to-night variability of both median and scatter of $\mathcal{L}_0$ is readily seen. The histogram of $\log\mathcal{L}_0$ for the whole mission is also presented. The $\mathcal{L}_0$ distribution is well approximated by a log-normal one. Its median is 24 m, and rms scatter of $\log\mathcal{L}_0$ is ±0.22, or ±1.67 times. A χ^2 test accepts log-normal distribution with a significance level of $P(\chi^2) = 0.24$.

On the night of August 29/30 the seeing and wavefront outer scale were simultaneously measured during 1 hour with the ADONIS adaptive optics system (Rigaut et al., 1991; Beuzit et al. 1994) on the ESO 3.6 m telescope. ADONIS worked in open-loop mode. Outer scale and seeing were calculated from the wavefront tilts recorded by the 7x7 element Shack-Hartmann sensor. A simplified method of $\mathcal{L}_0$ calculation was adopted. The AA variances on the individual wavefront sensor sub-apertures and on the full telescope aperture are computed. Their ratio is used to derive $\mathcal{L}_0$ by the approximate formula given by

Ziad et al. (1994). The simultaneous measurements of $\mathcal{L}_0$ with ADONIS and GSM are plotted in Fig. 5. There is no detailed correlation, which is quite natural because the distance between GSM and 3.6 m telescope was more than 1 km. However, the values of $\mathcal{L}_0$ found by both instruments agree well, and the temporal behaviour is also similar, as well as the measured seeing. This comparison proves that GSM data are indeed useful for the analysis and prediction of AO system performance.

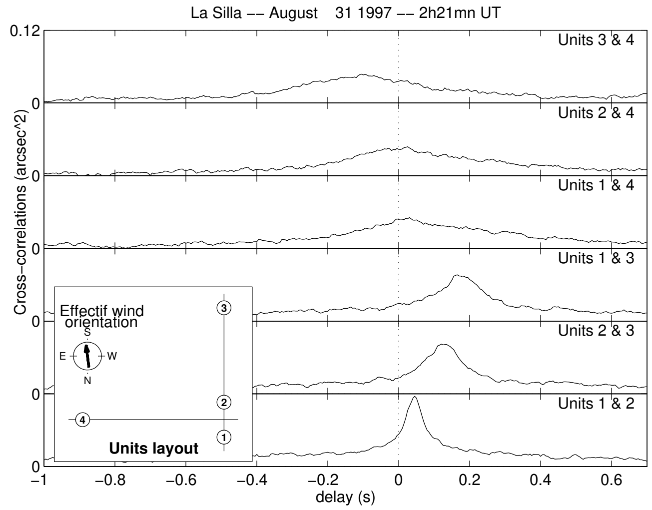

Fig. 6. Temporal cross-correlation functions of the angle of arrival fluctuations at the 6 baselines are plotted on the same scale. The displacement of their maximum is directly related to the projection of the effective wavefront speed onto a given baseline. The instrument configuration and the derived wind speed orientation are shown in the inset. The effective wind speed module is 5.8 m/s.

3.3. *Effective wind speed and AO time constant*

The temporal evolution of the perturbed wavefront is frequently considered in the framework of the "frozen turbulence" (Taylor) hypothesis, as a constant screen driven by the wind. The analysis of ADONIS data revealed that this situation does indeed occur at La Silla 15% of time (Gendron & Lena 1996). Although Taylor hypothesis remains a crude approximation of the reality, an effective wavefront speed can be introduced as some average C_n^2-weighted wind speed. Its component along each baseline can be computed either from the phase of the corresponding temporal cross power spectrum of AA fluctuations (Avila et al. 1997) or, equivalently, as a displacement of the AA cross-correlation function maximum. Here we use the second technique.

The method of effective wind speed measurement with GSM is illustrated in Fig. 6 where cross-correlation functions of AA are plotted for 6 baselines. From the time lag at each baseline it is found that wind speed was 5.8 m/s in the NNW direction (ground wind speed was 5.2 m/s from North). In this example, a single dominant layer obeying Taylor hypothesis provides a good overall description of temporal wavefront evolution. The corresponding AO time constant (Roddier et al. 1982) $\tau = 0.31 r_0/V$ is equal to 4.2 ms at $\lambda = 0.5$ nm.

4. Conclusions

The results of the first systematic monitoring of the wavefront outer scale at La Silla observatory are given. The GSM instrument also produces data on the seeing and effective wavefront velocity. In the near future the isoplanatic angle will be estimated as well, thus providing a complete set of spatial and temporal atmospheric parameters relevant to high angular resolution astronomy. The GSM instrument will be used during the next 2 years for testing several important sites, e.g. Paranal (Chile).

Acknowledgements. The authors would like to thank the La Silla staff for the efficient support of our mission, J.-L. Beuzit for assistance in ADONIS measurements, and all the people of Département d'Astrophysique de l'Université de Nice and of O.C.A. (Observatoire de la Cote d'Azur) who helped us to prepare this measurement campaign. Financial support for this work came from INSU (Institut National des Sciences de l'Univers), french M.E.N.R.T. (Ministère de l'Education Nationale, de la Recherche et de la Technologie), and from ESO (European Southern Observatory).

References

Agabi A., Borgnino J., Martin F. et al., 1995, A&AS 109, 557
Avila R., Ziad A., Borgnino J. et al., 1997, J. Opt. Soc. Amer. A14, 3037
Beuzit J.-L., Hubin N., Gendron E. et al., 1994, Proc. SPIE 2001, 955
Borgnino J., 1990, Appl. Opt. 29, 1863
Borgnino G., Martin F., Ziad A., 1992, Opt. Comm. 91, 267
Gendron E., Lena P., 1996, ApSS 239, 221
Loos G.C., Hogge C.B., 1979, Appl. Opt. 18, 2654
Martin F., Tokovinin A., Agabi A. et al., 1994, A&AS 108, 1
Rigaut F., Rousset G., Kern P. et al., 1991, A&A 250, 280
Roddier F., Effects of atmospheric turbulence in optical astronomy. In: Wolf E. (ed), Progress in Optics, North Holland, Amsterdam, 1981, p. 281
Roddier F., Gilli J.M., Lund G., 1982, J. Opt. (Paris) 13, 263
Sarazin M., Roddier F., 1990, A&A 227, 294
Voitsekhovich V.V., Cuevas S., 1995, J. Opt. Soc. Amer. A12, 2523
Ziad A., Borgnino J., Martin F,. Agabi A., 1994, A&A 282, 1021

This article was processed by the author using Springer-Verlag LaTeX A&A style file *L-AA* version 3.